



## Live Webinar Series: From Polar Pesticide Panels to Multiresidue Mega-Methods

This scientific eSeminar Series addresses pesticide analysis in food for panels of polar pesticides and how to successfully implement 'mega' methods for hundreds of residues, whilst adhering to the latest SANTE/ 11312/2021 guidelines.

### **Quantitative Analysis of 764 Pesticides in Tomato by LC/MS/MS**

Tuesday, 06 June 2023, 3:00 p.m. CEST

### **A Robust Method For the Sensitive Analysis of Non-Derivatized Polar Pesticides in Food by LC/MS/MS**

Wednesday, 14 June 2023, 3:00 p.m. CEST



See abstracts  
and register!

## RESEARCH ARTICLE

# Laser ablation mass spectrometry blast through detection in R

Alex Searle-Barnes  | James A. Milton | Christopher D. Standish  |  
Gavin L. Foster | Thomas H. G. Ezard

Ocean and Earth Science, University of Southampton, Southampton, UK

**Correspondence**

Alex Searle-Barnes, Ocean and Earth Science, University of Southampton, European Way, Southampton SO14 3ZH, UK.  
Email: [c.j.searle-barnes@soton.ac.uk](mailto:c.j.searle-barnes@soton.ac.uk)

**Funding information**

Natural Environment Research Council, Grant/Award Number: NE/P019269/1

**Rationale:** Organisms that grow a hard carbonate shell or skeleton, such as foraminifera, corals or molluscs, incorporate trace elements into their shell during growth that reflect the environmental change and biological activity they experienced during life. These geochemical signals locked within the carbonate are archives used in proxy reconstructions to study past environments and climates, to decipher taxonomy of cryptic species and to resolve evolutionary responses to climatic changes.

**Methods:** Here, we use laser ablation inductively coupled plasma mass spectrometry (LA-ICP-MS) as a time-resolved acquisition to quantify the elemental composition of carbonate shells and skeletons. We present the LABLASTER (Laser Ablation BLAST Through Endpoint in R) package, which imports a single time-resolved LA-ICP-MS analysis, then detects when the laser has ablated through the carbonate as a function of change in signal over time and outputs key summary statistics. We provide two examples within the package: a fossil planktic foraminifer and a tropical coral skeleton.

**Results:** We present the first R package that automates the selection of desired data during data reduction workflows. This is achieved by automating the detection of when the laser has ablated through a sample using a smoothed time series, followed by removal of off-target data points. The functions are flexible and adjust dynamically to maximise the duration of the desired geochemical target signal, making this package applicable to a wide range of heterogenous bioarchives. Visualisation tools for manual validation are also included.

**Conclusions:** LABLASTER increases transparency and repeatability by algorithmically identifying when the laser has either ablated fully through a sample or across a mineral boundary and is thus no longer documenting a geochemical signal associated with the desired sample. LABLASTER's focus on better data targeting means more accurate extraction of biological and geochemical signals.

## 1 | INTRODUCTION

Laser ablation inductively coupled plasma mass spectrometry (LA-ICP-MS) is a powerful analytical tool to quantify the elemental composition of a wide variety of natural and anthropogenic materials.

A laser beam is focussed to the surface of a target and then pulsed to ablate the sample. Particles from the ablated sample are subsequently transported into an inductively coupled plasma ionisation source then to a mass spectrometer for detection based on the mass-to-charge ratio, which can be converted into a time-resolved isotopic or

This is an open access article under the terms of the [Creative Commons Attribution](https://creativecommons.org/licenses/by/4.0/) License, which permits use, distribution and reproduction in any medium, provided the original work is properly cited.

© 2023 The Authors. *Rapid Communications in Mass Spectrometry* published by John Wiley & Sons Ltd.

elemental profile. LA-ICP-MS has become increasingly popular with biogenic carbonates, including foraminifera,<sup>1–3</sup> coral skeletons<sup>4</sup> and molluscs,<sup>5</sup> all of which act as archives of geochemical signals that can be used as proxy measurements to both reconstruct past environments and study the evolutionary response to long-term climate change.

Recent instrumentation advances enable LA-ICP-MS to collect trace element to calcium ratio (TE/Ca) results comparable to traditional solution based ICP-MS but with simpler sample preparation and higher throughput.<sup>6</sup> This solid sample and laser approach also allows for higher spatial resolution measurement of the sample and avoids the averaging of heterogeneity that occurs in solution-based ICP-MS. Nevertheless, there is no package for the R Environment for Statistical and Graphical Computing<sup>7</sup> that combines high data throughput with the additional nuance that laser ablation data processing requires to keep the maximum amount of relevant data. To fully leverage the gains of LA-ICP-MS, any software must be flexible enough to handle nonhomogeneous samples.

Some ready-to-use free computer packages exist to process LA-ICP-MS data such as elementR<sup>8</sup> or the discontinued LAICPMS,<sup>9</sup> both of which use the R environment, and LATools,<sup>10</sup> which uses the Python environment. ElementR provides a point-and-click graphical user interface that slows data reduction throughput while giving the user fine control over the data integration period. TERMITE<sup>11</sup> is not a package per se but is optimised for repeatable data reduction of homogenous samples, where the data integration period must be adjusted individually for each measurement and therefore requires manual validation.

These software packages provide a general end-to-end workflow to process experimental data into results rather than specialising on a particular data reduction step. In comparison, the LABLASTER package presented here contains a function that specialises in identifying when the laser is no longer recording the geochemical target of interest and is therefore designed for high-throughput processing that does not require user interaction once configured. A variety of endpoint detection mechanisms are used in the literature, including fixed time stamps,<sup>2</sup> k-means clustering,<sup>8</sup> analyte signal below a given threshold,<sup>12</sup> the mid-point between high and background signal counts<sup>10</sup> and even manual identification when the complexity of the samples is too great.<sup>10</sup> Here, we fit a function over a first derivative to calculate the rate of signal change. As LA-ICP-MS increases in popularity and experiments become more complex, there is a need for repeatable algorithmic protocols that can deal with heterogeneous samples or where repeat measurements may have different integration times.

Each discipline using LA-ICP-MS tends to measure samples that have different matrixes and properties, for example polished rock sections, pellets or carbonate shells. The examples presented here have been tailored to the field of ecology and evolution with a fossilised planktic foraminifer and the field of paleoclimate geochemistry with a tropical coral skeleton. The LABLASTER package will work with any sample that the laser may ablate through (or past) and hit an undesired target of different elemental composition. The foraminifera example here demonstrates how LABLASTER can be

used to meet the specific needs of micro-palaeontologists, whose data are often skewed and highly variable.<sup>8</sup>

At any given time, a single species may contain individuals that have highly variable trace element signals within their shells due to the presence of subspecies, ontogenetic trends and/or lived environment. Comparisons of geochemical signals within a species can untangle and quantify the magnitude of such variability, as exemplified by Kearns et al., who used Mg/Ca ratios of the extant foraminifera species *Globigerinoides ruber* measured by LA-ICP-MS to distinguish between depth habitats and thus inhabited niches of the distinct subspecies. Analysing trace element signals is one technique to identify temperature-differentiated niches that underpin many theoretical ecological, evolutionary and eco-evolutionary models.<sup>13</sup>

Here, we (1) improve current processing capabilities by dynamically identifying the end of the sample of a carbonate subject and (2) implement this improved processing in the first freely available software to automate data extraction of a time-resolved elemental depth profile. As demonstrated in the examples below, the end of the sample may be the maximum depth at a single spot location for a shell or a pore in a linear profile of a coral skeleton, but any nonhomogeneous target sample is generally applicable.

An automated laser ablation setup often requires a constant firing time to be programmed into the controlling computer, with no regard for the heterogeneity or variation in thickness of the target. When samples are porous or have changes in mineralogy or variation in thicknesses within a single analytical session while using a consistent laser pulsing time, there is inevitably a chance that the laser will move across a mineral boundary or ablate through the entire depth of the sample, and thus the recorded data will not be restricted to only the area of interest. Any elemental measurement recorded after the laser has ablated through the sample is not of the target, and it should be removed before subsequent statistical analysis. Because the time taken to ablate through a sample is not consistent, such corrections can be made manually on an ad hoc basis, but additional manual handling would be time-consuming, laborious and prone to subjective differences among operators. There are clear methodological benefits from the development of a repeatable workflow.

The LABLASTER package works alongside elementR or TERMITE application or can be run as a standalone process within bespoke scripts, providing a flexible and versatile methodological improvement for heterogeneous samples that treats each sample individually to optimise signal-noise ratios. LABLASTER can batch process within a workflow, is customisable to the sensitivity for endpoint detection and does not require a point-and-click user interface. These features offer a higher throughput for data reduction compared to manual or alternative software methods and maximise retainment of on-target data for subsequent analysis.

## 2 | MATERIALS AND METHODS

The LABLASTER package contains one function named `endPoint()` that calculates four items and four example data sets to illustrate its

use, including the foraminifer and coral examples presented here. The package requires R ( $\geq 3.5.0$ )<sup>7</sup> and has a number of dependencies as it calls functionality from the `stats`,<sup>7</sup> `smooth`,<sup>14</sup> `ggplot2`, `magrittr`<sup>15</sup> and `scales`<sup>16</sup> packages.

## 2.1 | endPoint detection

The main function of the LABLASTER package is to detect when the laser has either ablated through a target (e.g. a carbonate shell or coral skeleton) or across a mineral boundary in a transect. In the following sections, we illustrate this behaviour on a planktic foraminifer and a tropical coral as case studies.

Identifying the time range in which the laser is ablating the target is essential for accessing and correlating the relevant data within the recorded time series. The LABLASTER package assumes the data frame supplied begins with the laser in focus of the desired target and the `endPoint()` function determines the time stamp when the laser has ablated through the sample or across a boundary where the isotope signal changes rapidly. Keeping only the data between the start time and end time focusses subsequent analysis on only relevant target data.

### 2.1.1 | Algorithm

The `endPoint()` function requires a single data frame containing a minimum of two columns: a column containing a time index and a column containing isotope signal counts. This data frame is supplied to the function as the argument `detectDf` with the time index column specified as `timeCol` and the isotope signal column specified as `signalCol`. Any element that is abundant within the target but is scarce in the surrounding medium could be used to detect the ablate through endpoint time. In the case study below we use 'Ca44' containing the <sup>44</sup>Ca isotope counts per second as the `signalCol` as this is abundant within the foraminifera test and therefore shows high counts when the laser is focussed and on target, but once the laser has ablated through the chamber wall, it becomes defocussed, and therefore the measured counts decrease. The function expects for the first row of the supplied data frame to have the laser on-target.

The algorithm of the `endPoint` function first calculates a simple moving average over the `signalCol` isotope counts, with the number of points in the moving average controlled by the `smoothing` argument. This smoothed isotope count signal is then scaled between 0 and 1 to provide consistency within subsequent algorithm steps, making this function more generic and applicable to all time-resolved acquisition mass spectrometry data. A larger amount of smoothing reduces the variance between adjacent data points, averaging out any signal spikes and therefore flattening the signal against time curve. A flatter time-resolved profile curve gives greater distinction between the elevated signal of desired target ablation and the lower signal of the undesired under- or adjacent target surface.

Using smoothing to de-spike and flatten the signal during the time of elevated signal reduces the magnitude of variance over time and therefore reduces the likelihood of a false-positive detection in a change of ablated material composition, which is used as part of the detection in later steps of the algorithm. Over-smoothing the signal reduces the distinction from a sudden signal drop to a shallower gradual drop between the higher on-target and the lower off-target signal intensities that the algorithm uses to detect that the laser is no longer ablating the desired target, causing a delayed detection. Over-smoothing can be identified manually using the visualisation tools by comparing the black-scaled smoothed signal and blue-scaled rate of signal change ( $dy/dt$ ) lines.

Next, the algorithm calculates the number of data points per time step in the data frame supplied. The temporal resolution of the data can affect how sensitive the algorithm is to the rate of scaled signal change. The algorithm uses a moving window to calculate the rate of change in signal against time. Higher temporal resolution data can result in a smoother decline in isotope signal across the default time window, causing a delayed endpoint detection, therefore using a wider time window captures a larger magnitude signal drop. The algorithm uses the largest magnitude of negative rate of isotope signal change to identify that the laser is no longer well focussed on the desired target. Without a rapid signal drop, for example, if the laser did not fully ablate through the target or no mineral boundary was crossed, then the algorithm will return the final observation in the provided data frame and a warning message is displayed to encourage use of the manual validation tools to check the results. The number of data points used as the width of the moving window is controlled by the `dt` argument. The minimum number of data points required to detect the endpoint is  $dt + 2$ .

Once the algorithm has identified the largest magnitude of negative rate of smoothed signal change, the corresponding time stamp is identified. As the largest signal drop occurs shortly after the laser has ablated through the sample or crossed a boundary, it is necessary to also remove the data that occurs between the final data point when the laser was on target and the largest signal drop. This elapsed time is calculated by dividing the moving window width by the number of data points per time step and is subtracted from the signal change time stamp. This earliest time stamp is when the laser was last ablating on the desired target and is returned as a numeric value in the returned data frame.

```
library(lablaster)
endPoint(detectDf, timeCol = "Time", signalCol = "Ca44", smoothing = 5,
         dt = 10, profile = "FALSE", timeUnits = "seconds")
```

## 2.2 | Visualisation of the blast through algorithm

The `endPoint` function additionally provides visualisation tools into the mechanism of the algorithm. The smoothed scaled signal, rate of change and inferred bounds on the geochemical target are useful for

diagnosing the real-life efficacy. A `ggplot2` object is generated when the `profile` argument is set to `TRUE`. If the `profile` argument is `TRUE`, then the time units of the analysis are also required and specified with the `timeUnits` argument.

## 2.3 | Returned values

The `endPoint` function returns a single data frame containing the values calculated.

`$startTime` contains the earliest time step in the supplied time-resolved acquisition as a numerical value.

`$endTime` contains the last time step before the laser ablated through the carbonate shell as described above.

`$df` contains the supplied data frame with the raw data but containing only the rows that occur that are identified as on-target and three additional columns that were calculated by the algorithm of (1) the smoothed `signalCol`, (2) scaled rate of change and (3) the scaled smoothed `signalCol`.

`$profile` contains a visualisation of the endpoint mechanism as described above. This is only available if a profile was generated using `profile = 'TRUE'`.

## 3 | CASE STUDY

### 3.1 | A foraminifer setup

#### 3.1.1 | Experimental setup

A single planktonic foraminifer case study is included in the package as a worked example. Planktonic foraminifera are unicellular zooplankton distributed throughout the world's oceans as a key resource in understanding the Earth's climate system.<sup>2,3</sup> Foraminifera grow connected chambers throughout their life with those in the final whorl accessible for LA-ICP-MS analysis<sup>17</sup> (Figure 1). The thickness of a foraminifera chamber wall can vary substantially even within an individual. Some have thick solid chamber walls, while others have a highly porous structure as a result of species-level morphological variations, biological controls and environmental influences. This natural variability is the motivation for our development of automated processing methods and thus better control of geochemical 'vital effects'.<sup>18</sup> The case study is from the antepenultimate chamber of *Menardella exilis* foraminifera 72, identified hereon as 'Foram-72-shot-3'. The aim of this experiment was to quantify how Mg/Ca ratios vary between and within individual foraminifera.

The experimental setup is described fully in Kearns et al. Briefly, major and trace elements in the foraminifera test were analysed using a New Wave UP193 laser ablation system (ArF source, 30  $\mu\text{m}$  spot diameter, fluence of 0.73 J/cm<sup>3</sup> and 5 Hz pulse rate) coupled to an Agilent 8900 triple quadrupole inductively coupled plasma (ICP-QQQ) mass spectrometer in single quadrupole mode using a He and Ar gas

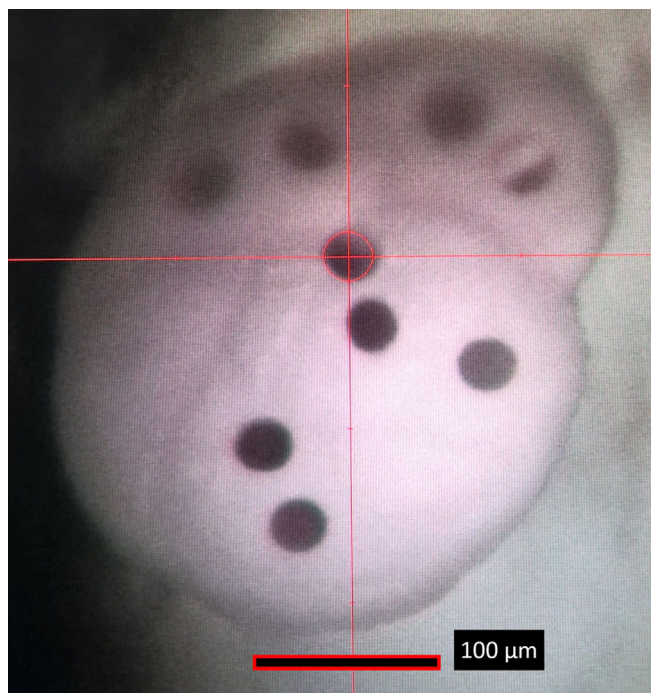


**FIGURE 1** LA-ICP-MS holes from each shot are visible in the laser system software. [Color figure can be viewed at [wileyonlinelibrary.com](http://wileyonlinelibrary.com)]

mixture (900 mL/min) at the University of Southampton. Each laser spot pattern was sequenced with a 30 s warmup, 50 s laser pulse and 30 s washout. The default values within this `endPoint` function are based on outputs from this setup.

Initial processing of the time-resolved acquisition data was performed within R.<sup>7</sup> The first 30 s was used to calculate the background signal and then removed. The next 5 s was removed as the isotopic signal began to rise due to the laser firing, but the ablated material was still travelling through the system. As our washout time was enough to purge the system after each analysis, the duration of this signal rise was regular and reproducible.

#### 3.1.2 | `endPoint` detection function

The data frame containing the background-corrected remainder of the acquisition (Figure 2B) was supplied to the `endPoint` function. With the first 35 s removed, we ensured that the laser was firing on the foraminifera's outer test wall and the ablated material was reaching the mass detector for the first row in the data frame supplied. In this example, we use the <sup>44</sup>Ca isotope measurements due to the high signal:noise ratio and the abundance of <sup>44</sup>Ca within the foraminifera test, which provides greater distinction between higher signal counts for the duration when the laser was on target and lower signal counts when the laser was ablating the glass slide mount. The `endPoint` function was used to dynamically identify the time step when the laser had fully ablated through the foraminifera

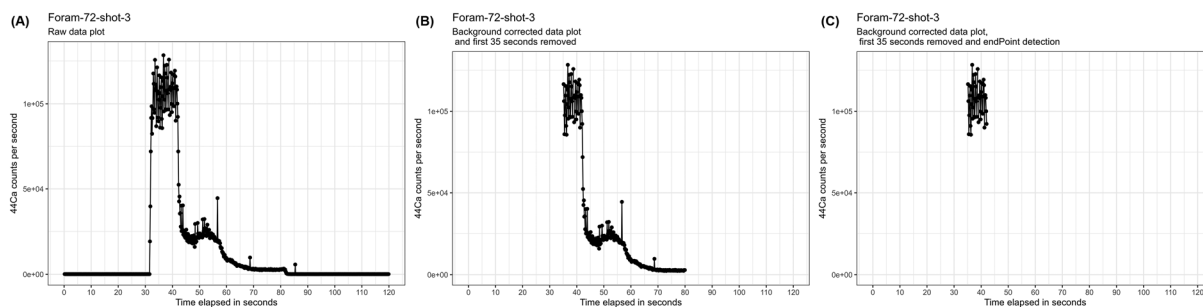


**FIGURE 2** The processes implemented in the endPoint function in a time-resolved acquisition of Foram-72-shot-3 as a visualisation of the returned data frame \$df. (A) shows the entire raw  $^{44}\text{Ca}$  data collected, (B) shows the background-corrected  $^{44}\text{Ca}$  with the first 35 s removed as this was before the laser was turned on and the ablated material is still travelling through the system and this is the data frame passed into the endPoint function, and (C) shows the target data retained after running the endPoint function, with both the first 35 s and post endPoint detection  $^{44}\text{Ca}$  data removed.

### Example data Foram-72-shot-3

With a smoothing of 5 observations, a  $dt$  of 10 observations and  $dt/\text{scanRate}$  of 1.561 seconds

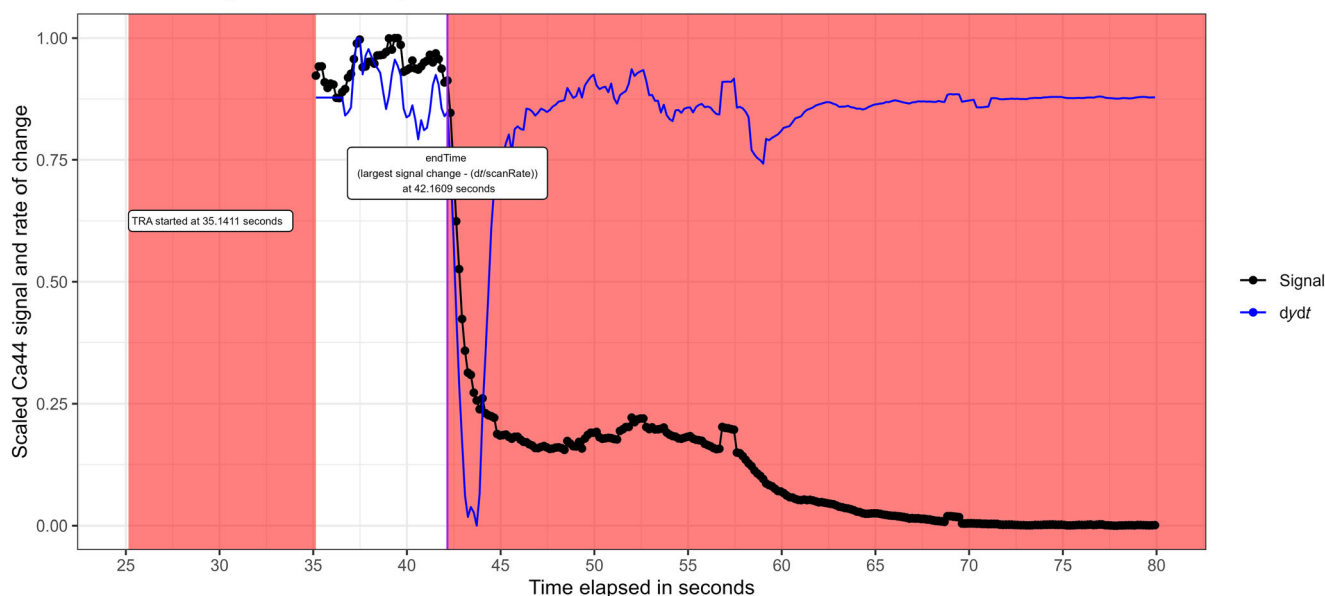


**FIGURE 3** A visualisation of the endPoint function for the Foram-72-shot-3 case study, showing the scaled smoothed  $^{44}\text{Ca}$  signal in black, the scaled rate of signal change in blue and the shaded red areas that identify the data point rows that are removed in the returned data frame. [Color figure can be viewed at [wileyonlinelibrary.com](http://wileyonlinelibrary.com)]

test and to keep only the observations while the laser was ablating the target (Figure 2C).

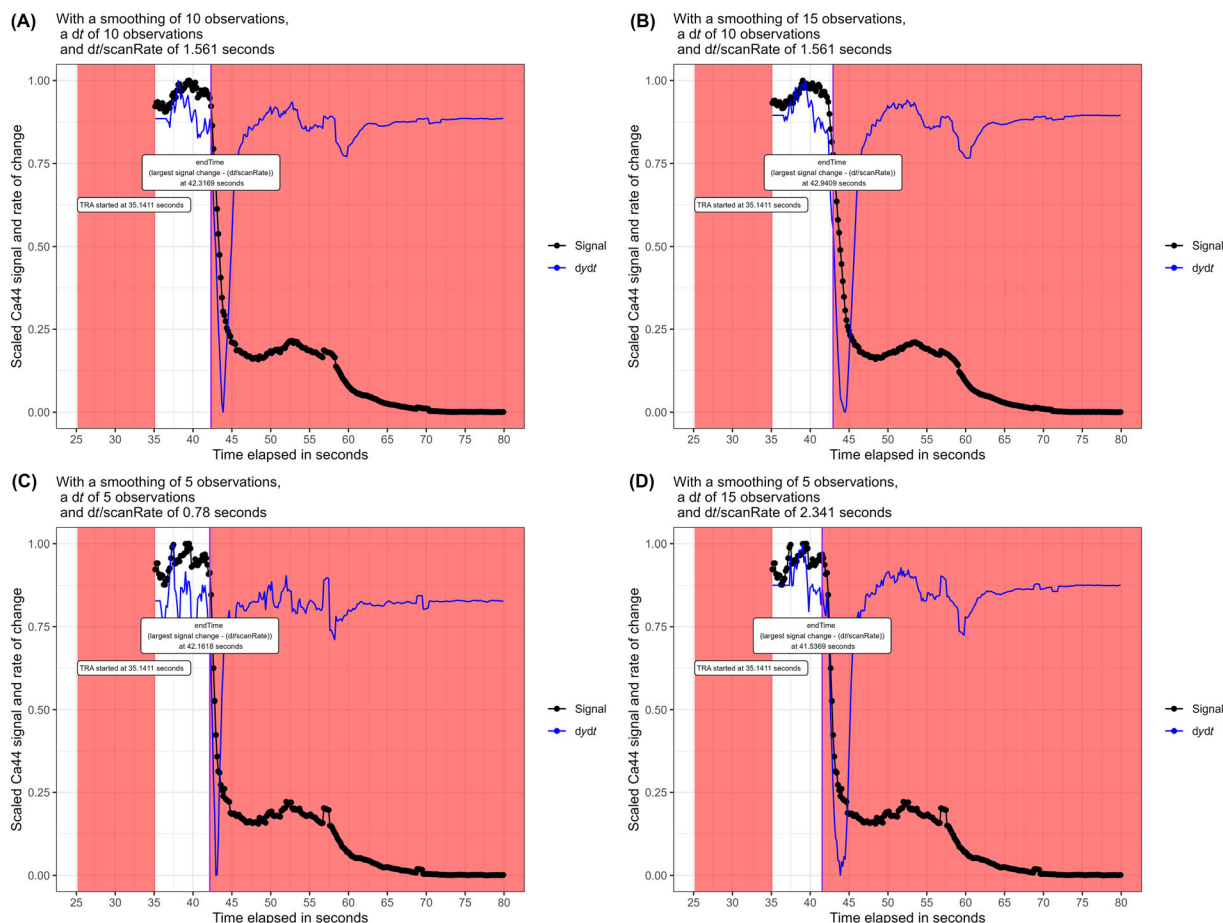
```
endPoint(detectDf = foram72shot3, dt = 10, smoothing = 5, timeCol =
"Time", signalCol = "Ca44", profile = "TRUE", timeUnits =
"seconds")
```

Figure 3 shows the manual validation tools to check that the endPoint function had successfully identified when the laser had ablated through the entire depth of the test wall. The black line is a scaled transformation of the smoothed signal specified in signalCol,

the blue line is the scaled rate of change in signal over the moving time window and the shaded red areas identify the data points removed from the returned data frame, \$df, as these exceed the endpoint blast through detection time stamp.

### 3.1.3 | Comparison of endpoint detection by varying the smoothing and dt arguments

We repeated the endpoint detection of the Foram-72-shot-3 case study specifying alternative smoothing and dt arguments (Figure 4). In comparison to Figure 3, which uses the default smoothing and dt



**FIGURE 4** Comparison of endpoint detection of Foram-72-shot-3 by varying the smoothing and  $dt$  arguments. Using the default values of smoothing = 5 and  $dt = 10$  the endpoint is identified as 42.0 s, in comparison to (A) smoothing = 10 and  $dt = 10$  results with endpoint at 42.3 s, (B) smoothing = 15 and  $dt = 10$  results with endpoint at 43.6 s, (C) smoothing = 5 and  $dt = 5$  results with endpoint at 42.3 s, and (D) smoothing = 5 and  $dt = 15$  results with endpoint at 41.7 s. [Color figure can be viewed at [wileyonlinelibrary.com](http://wileyonlinelibrary.com)]

values, a larger smoothing value delays the endpoint detection, whereas larger  $dt$  values decrease the number of data points that are considered on-target. The user should use the visualisation tools to confirm the `endPoint()` function is optimised for any given application by keeping the maximum on-target data. Excessive smoothing returns additional rows of data when the laser is no longer on-target or an excessive  $dt$  returns a premature endpoint time stamp and on-target data are unnecessarily removed. In our experience, and with this particular application, examining five profiles was sufficient to identify the optimal smoothing parameter.

### 3.1.4 | Comparison without using `endPoint` detection

Foraminifera are archives of geochemical signals that are used in proxy measurement reconstructions. Sea surface temperatures can be reconstructed with calibrated equations using a ratio of magnesium to calcium as an input, making this Mg/Ca (mmol/mol) a popular

geochemical measurement.<sup>3,6</sup> Our particular research concerns using trace element ratios in foraminifera to explore speciation events, tracking how new species and subspecies occupy the environment differently to their ancestors.<sup>18,19</sup> As a result, we typically analyse many individual foraminifera with multiple laser spots on each chamber (e.g. in Kearns et al.).

When processed without identifying the endpoint, the analysis time was between 35 and 80 s elapsed resulting with the median  $^{24}\text{Mg}/^{44}\text{Ca}$  ratio of Foram-72-shot-3 as  $4.37 \pm 2.10$  mmol/mol. In contrast, when processed with the `endPoint()` function, the analysis time was between 35 and 41 s elapsed resulting with the median of  $2.46 \pm 1.35$  mmol/mol. While the signal counts of both Mg and Ca decrease as more time elapses due to laser defocussing and ablation through the carbonate structures (Figure 3), their ratio increases in this case. Lower absolute counts also increase uncertainty in the calculated ratios; hence, the use of the `endPoint()` function increases both accuracy (by focussing on the geochemical target) and precision through using higher-quality sample data for statistical analysis.

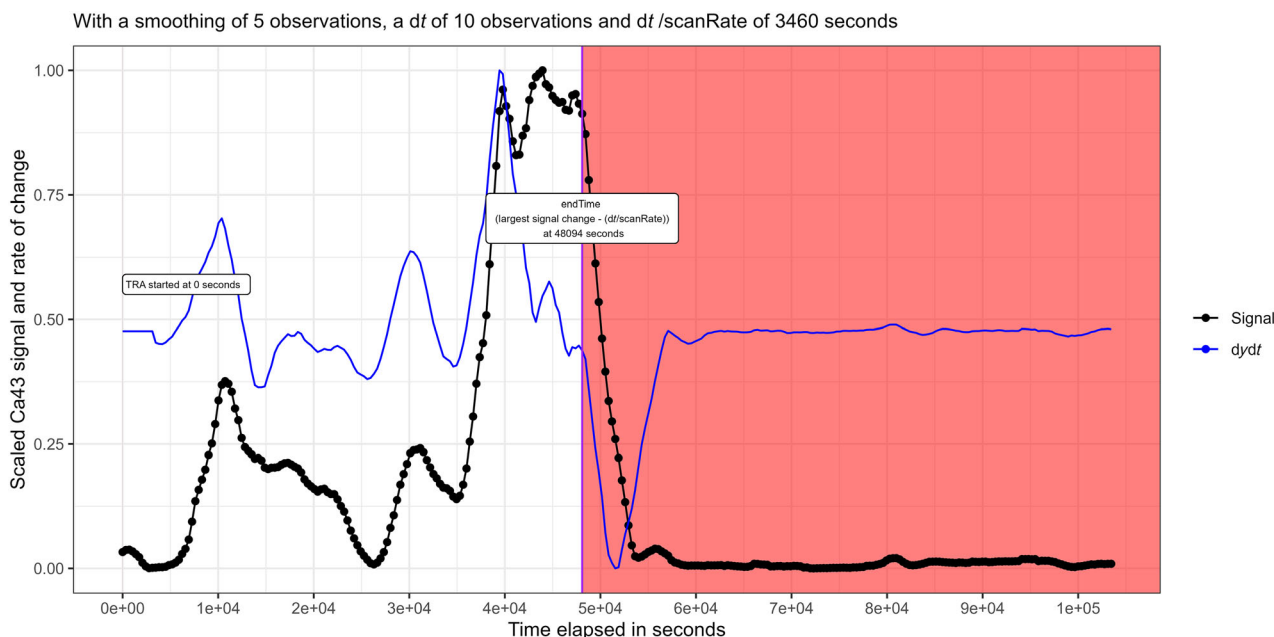


**FIGURE 5** A visualisation of the endPoint function for the Coral-6 case study, showing the scaled smoothed  $^{43}\text{Ca}$  signal in black, the scaled rate of signal change in blue and the shaded red areas identifying the data point rows that are removed in the returned data frame. [Color figure can be viewed at [wileyonlinelibrary.com](http://wileyonlinelibrary.com)]

## 3.2 | A coral example

### 3.2.1 | Experimental setup

A transect across a sample of tropical coral *Acropora polystoma*, cultured in artificial seawater in a closed coral mesocosm at the Coral Reef Laboratory, National Oceanography Centre, Southampton,<sup>20</sup> is also included in the package as an example of an ablation line and is identified hereon as 'coral-6'. As polished coral sections can be irregular in shape, thickness and porosity, it is possible for the laser to ablate fully through at a thinner location or traverse a boundary between the sample and its mounting resin. In this example, the ablation line passes over a thinner section of coral and consequently the laser fully ablates through before the end of the analysis time.

### 3.2.2 | endPoint detection function

This coral section has bands of higher and lower calcium concentration across the laser transect and consequently fluctuating higher and lower counts for the calcium signal are observed. In this example, we selected the dt and smoothing parameters to de-spike these real signal fluctuations and using the included manual visualisation tool (Figure 5) to validate our selection identified the moment when the laser fully ablated through the coral. In this analysis,  $^{43}\text{Ca}$  was the calcium isotope measured and hence used for endpoint detection.

```
endPoint(detectDF = coral6, dt = 10, smoothing = 5, timeCol =
"Time", signalCol = "Ca43", profile = "TRUE", timeUnits =
"seconds")
```

## 4 | CONCLUSION

While LA-ICP-MS has many benefits over traditional solution-based ICP-MS methods for measuring major and trace elements in various carbonate objects, current analytical setups can be inflexible with regards to laser firing duration. Our freely available LABLASTER package implements methodological improvements to refine analytical workflows. We plan to extend endPoint() functionality to also include a startPoint() equivalent to detect when the laser starts pulsing on the desired target.

The endPoint function that implements these improvements is compatible for use within loops, aiding high-throughput and repeatable data cleaning of carbonate materials that are ubiquitously used in past climate reconstructions, geochemical ecology and evolution studies, and subspecies taxonomic distinctions.

### AUTHOR CONTRIBUTIONS

Alex Searle-Barnes designed the functions and wrote the code. James A. Milton and Gavin L. Foster provided methodological support and laboratory analysis. Christopher D. Standish provided the coral data for additional algorithm testing and example data published within the LABLASTER package. Thomas H. G. Ezard validated the functions and code. Alex Searle-Barnes drafted the manuscript,



and James A. Milton, Gavin L. Foster, Christopher D. Standish and Thomas H. G. Ezard provided comments on earlier drafts.

## ACKNOWLEDGMENTS

This work was supported by Natural Environment Research Council award NE/P019269/1.

## CONFLICT OF INTEREST STATEMENT

The authors do not declare a conflict of interest.

## DATA AVAILABILITY STATEMENT

The data that support the findings of this study are openly available in lablaster at <https://github.com/alexsb1/lablaster>.

## ORCID

Alex Searle-Barnes  <https://orcid.org/0000-0003-0389-7717>

Christopher D. Standish  <https://orcid.org/0000-0002-9726-295X>

## PEER REVIEW

The peer review history for this article is available at <https://www.webofscience.com/api/gateway/wos/peer-review/10.1002/rcm.9533>.

## REFERENCES

- Fehrenbacher JS, Spero HJ, Russell AD, Vetter L, Eggins S. Optimizing LA-ICP-MS analytical procedures for elemental depth profiling of foraminifera shells. *Chem Geol.* 2015;407-408:2-9. doi:10.1016/j.chemgeo.2015.04.007
- Hathorne EC, Alard O, James RH, Rogers NW. Determination of intratest variability of trace elements in foraminifera by laser ablation inductively coupled plasma-mass spectrometry. *Geochem Geophys Geosyst.* 2003;4(12). doi:10.1029/2003GC000539
- Eggins S, De Deckker P, Marshall J. Mg/Ca variation in planktonic foraminifera tests: Implications for reconstructing palaeo-seawater temperature and habitat migration. *Earth Planet Sci Lett.* 2003; 212(3-4):291-306. doi:10.1016/S0012-821X(03)00283-8
- Chalk TB, Standish CD, D'Angelo C, Castillo KD, Milton JA, Foster GL. Mapping coral calcification strategies from in situ boron isotope and trace element measurements of the tropical coral *Siderastrea siderea*. *Sci Rep.* 2021;11(1):472. doi:10.1038/s41598-020-78778-1
- Schöne BR, Zhang Z, Radermacher P, et al. Sr/Ca and Mg/Ca ratios of ontogenetically old, long-lived bivalve shells (*Arctica islandica*) and their function as paleotemperature proxies. *Palaeogeogr Palaeoclimatol Palaeoecol.* 2011;302(1-2):52-64. doi:10.1016/j.palaeo.2010.03.016
- Fehrenbacher J, Marchitto T, Spero HJ. Comparison of laser ablation and solution-based ICP-MS results for individual foraminifer Mg/Ca and Sr/Ca analyses. *Geochem Geophys Geosyst.* 2020;21: e2020GC009254. doi:10.1029/2020GC009254
- R Core Team. 2022. R: a language and environment for statistical computing. <https://www.R-project.org/>: R Foundation for Statistical Computing.
- Siroc C, Ferraton F, Panfili J, Childs A-R, Guilhaumon F, Darnaude AM. elementr: an R package for reducing elemental data from LA-ICPMS analysis of biological calcified structures. *Methods Ecol Evol.* 2017;8(12):1659-1667. doi:10.1111/2041-210X.12822
- Rittner M, Müller W. 2D mapping of LA-ICPMS trace element distributions using R. *Comput Geosci.* 2012;42:152-161. doi:10.1016/j.cageo.2011.07.016
- Branson O, Fehrenbacher JS, Vetter L, Sadekov AY, Eggins SM, Spero HJ. LAtools: a data analysis package for the reproducible reduction of LA-ICPMS data. *Chem Geol.* 2019;504:83-95. doi:10.1016/j.chemgeo.2018.10.029
- Mischel SA, Mertz-Kraus R, Jochum KP, Scholz D. TERMITE: an R script for fast reduction of laser ablation inductively coupled plasma mass spectrometry data and its application to trace element measurements. *Rapid Commun Mass Spectrom.* 2017;31(13): 1079-1087. doi:10.1002/rcm.7895
- Fricker MB, Kutscher D, Aeschlimann B, et al. High spatial resolution trace element analysis by LA-ICP-MS using a novel ablation cell for multiple or large samples. *Int J Mass Spectrom.* 2011;307(1-3):39-45. doi:10.1016/j.ijms.2011.01.008
- Ward BA, Collins S. Rapid evolution allows coexistence of highly divergent lineages within the same niche. *Ecol Lett.* 2022;25(8): 1839-1853. doi:10.1111/ele.14061
- Svetunkov I, Petropoulos F. Old dog, new tricks: a modelling view of simple moving averages. *Int J Prod Res.* 2018;56(18):6034-6047. doi: 10.1080/00207543.2017.1380326
- Wickham H, Averick M, Bryan J, et al. Welcome to the Tidyverse. *J Open Source Softw.* 2019;4(43):1686. doi:10.21105/joss.01686
- Wickham H., Seidel D. Scales: Scale functions for visualization. 2022. <https://scales.r-lib.org>
- Lea DW, Mashiotta TA, Spero HJ. Controls on magnesium and strontium uptake in planktonic foraminifera determined by live culturing. *Geochim Cosmochim Acta.* 1999;63(16):2369-2379. doi:10.1016/S0016-7037(99)00197-0
- Kearns LE, Searle-Barnes A, Foster GL, Milton JA, Standish CD, Ezard THG. The influence of geochemical variation among *Globigerinoides ruber* individuals on paleoceanographic reconstructions. *Paleoceanogr Paleoclimatol.* 2023;38:e2022PA004549. doi:10.1029/2022PA004549
- Steinke S, Chiu H-Y, Yu P-S, et al. Mg/ca ratios of two *Globigerinoides ruber* (white) morphotypes: Implications for reconstructing past tropical/subtropical surface water conditions. *Geochem Geophys Geosyst.* 2005;6(11). doi:10.1029/2005GC000926
- D'angelo C, Wiedenmann J. An experimental mesocosm for long-term studies of reef corals. *J Mar Biol Assoc UK.* 2012;92(4):769-775. doi: 10.1017/S0025315411001883

**How to cite this article:** Searle-Barnes A, Milton JA, Standish CD, Foster GL, Ezard THG. Laser ablation mass spectrometry blast through detection in R. *Rapid Commun Mass Spectrom.* 2023;37(15):e9533. doi:10.1002/rcm.9533